Evidence for a Spin Emulsion

P. M. Bentley*
Institut Laue-Langevin, 6 rue Jules Horowitz, 38042 Grenoble Cedex 9, France

R. Cywinski
School of Applied Sciences, University of Huddersfield, Huddersfield, HD1 3DH, United Kingdom
(Received 8 July 2008; published 26 November 2008)

Magnetic small-angle neutron scattering from the itinerant electron magnet, $Y(Mn_{1-x}Fe_x)_2$, in which ferromagnetic and antiferromagnetic spin correlations compete, is found to follow an anomalous Q^{-6} dependence ($Q = 4\pi \sin\theta/\lambda$). It is suggested that this scattering is the magnetic analogue of that predicted for a structural microemulsion by Teubner's extension of conventional Kirste-Porod scattering to well-defined interfaces with extreme differences between mean and Gaussian curvatures. The ''spin-emulsion-like'' morphology of magnetic interfaces in $Y(Mn_{1-x}Fe_x)_2$ is confirmed both qualitatively and quantitatively by a simple model based upon reported near neighbor Mn and Fe spin correlations.

DOI: 10.1103/PhysRevLett.101.227202 PACS numbers: 75.10.Nr, 61.05.fg, 75.50.Lk

For almost four decades small-angle neutron scattering (SANS) has provided invaluable insights into the evolution of spin correlations, cluster growth, and critical scaling in the vicinity of the critical concentration for long range magnetic order in percolating systems. In most cases the Q ($= 4\pi \sin\theta/\lambda$) dependence of the observed magnetic SANS intensity can be represented either by a simple Lorentzian function, associated with Ornstein-Zernicke-like critical scattering, or by a combination of Lorentzian plus squared-Lorentzian scattering, e.g.,

$$I(Q) = \frac{A}{\kappa^2 + Q^2} + \frac{B}{(\kappa^2 + Q^2)^2}, \quad (1)$$

in which κ is the inverse correlation range, and the second term is generally attributed to the effects of either random magnetic exchange or random anisotropy [1].

However, most of the prepercolative and percolative magnetic systems that have been studied using SANS to date are relatively simple alloys and compounds in which the exchange interactions are predominantly ferromagnetic. In contrast, we were interested to explore the nature and growth of spin correlations in a structurally homogeneous itinerant electron magnet in which competing ferromagnetic and antiferromagnetic correlations might play a significant role in defining the size and morphology of percolation clusters close to the critical concentration for ferromagnetism.

The $C15$ Laves phase system, $Y(Mn_{1-x}Fe_x)_2$, was selected as an appropriate model for the SANS study. The parent compound, YMn_2, is Pauli paramagnetic at high temperatures, with a magnetic response dominated by antiferromagnetically correlated longitudinal spin fluctuations [2]. On cooling to $T_N = 100$ K the manganese moments spontaneously localize and there is a discontinuous transition to an antiferromagnetically ordered state accompanied by a 5% volume expansion. The manganese moments (of $2.8\mu_B$) occupy a tetrahedral sublattice leading to magnetic frustration, relieved in part by the formation of a complex antiferromagnetic helix and partly by a modest tetragonal distortion [3].

Numerous studies have shown that the stability of the Mn moment and correspondingly the discontinuous transition to the magnetically ordered, expanded state is extremely sensitive to interatomic spacing. For example, hydrostatic pressure of only 3 kbar is sufficient to suppress moment formation, long range order, and the volume expansion [4]. Similarly, the chemical pressure resulting from 2.5 at. % substitution of iron at the manganese sites causes a collapse of the manganese moment and a return to a Pauli paramagnetic, antiferromagnetically correlated, spin fluctuating state [5]. With further additions of iron the transition metal moments appear to relocalize, giving rise first to a spin glass state and ultimately to ferromagnetic order beyond a percolation threshold of approximately $x_c \sim 0.3$.

Band structure calculations [6] and NMR measurements [7,8] on $Y(Mn_{1-x}Fe_x)_2$ at these intermediate concentrations indicate an inhomogeneous magnetic environment arising from mixed spin correlations: for an iron atom with fewer than three manganese atoms in its near-neighbor shell, the surrounding manganese spins are oriented parallel to that of the iron atom (i.e., local ferromagnetism) while for an iron atom with four or more manganese near neighbors there is an enhancement of the iron moment and the surrounding manganese spins are aligned antiparallel to that of the iron atom (i.e., local antiferromagnetism).

The SANS experiments were carried out on a range of $Y(Mn_{1-x}Fe_x)_2$ compounds with $0.2 \leq x \leq 0.6$ spanning the percolation threshold. The measurements were performed on the D11 instrument at the Institut Laue Langevin, Grenoble. SANS spectra were collected over a

wide temperature range and the magnetic scattering was isolated by subtracting a temperature independent background scattering associated with nuclear defects and measured at high temperatures. This is standard practice in systems with no structural transition [9]. The low-temperature structural anomalies in this system disappear along with the antiferromagnetism at around $x \sim 0.025$ [5].

In Fig. 1 we show the resulting temperature dependent magnetic SANS for several values of Q for the $x = 0.6$ sample. At higher Q values evidence of critical scattering is seen at temperatures close to 250 K (i.e., the Curie point [10]), while at lower Q the scattering is dominated by a rapid increase in intensity towards low temperatures.

We find that the Q dependence of the SANS is significantly different from that generally observed for magnetically inhomogeneous, percolative systems and is inconsistent with the generalized SANS function of Eq. (1): it is evident from Fig. 2 that the Q dependence of the SANS intensity from $Y(Mn_{0.4}Fe_{0.6})_2$ follows a precise but anomalous Q^{-6} dependence at lower temperatures. Similar behavior is also observed for other $Y(Mn_{1-x}Fe_x)_2$ compounds with $0.2 \leq x \leq 6$. For all of these samples the SANS exhibits a Q dependence proportional to Q^{-x} with $x > 4$. At the lowest measured temperatures, the relative contribution from the Q^{-6} term to the SANS increases with Fe concentration, and is greatest for $Y(Mn_{0.4}Fe_{0.6})_2$.

Small-angle intensity which follows a power law higher than the inverse fourth power in Q is extremely unusual. Q^{-4} dependence, generally known as Porod scattering [11,12], arises from sharply defined surfaces and "fuzzy" Porod scattering [13] associated with less well-defined interfaces can lead to even more pronounced Q dependences with $I(Q) \sim Q^{4+\beta}$. Similar scattering is also observed from fractal surfaces, for which $\beta = (2 - D)$ where D is the fractal dimensionality. However, for both fuzzy Porod scattering and fractal surfaces β is always found experimentally and theoretically to be less than 2 [13,14].

To explain the anomalous Q^{-6} dependence of the SANS from $Y(Mn_{0.4}Fe_{0.6})_2$ it is necessary to turn to Teubner's [15] rigorous and concise derivation of Porod surface scattering and its related second order component, generally known as Kirste-Porod scattering [16], for systems such as bicontinuous microemulsions in which the interface surfaces are extremely thin but smooth. Teubner's analysis predicts that higher powers of Q may arise in SANS because of the curvature of these scattering surfaces, i.e.,

$$I(Q) \propto \frac{1}{Q^4} + \frac{1}{Q^6}\left(\frac{3}{2}\langle H^2\rangle - \frac{1}{2}\langle K\rangle\right), \qquad (2)$$

where H and K are the mean and Gaussian curvatures of the scattering surface, respectively. These are related directly to the principal curvatures k_1 and k_2, i.e., the maxi-

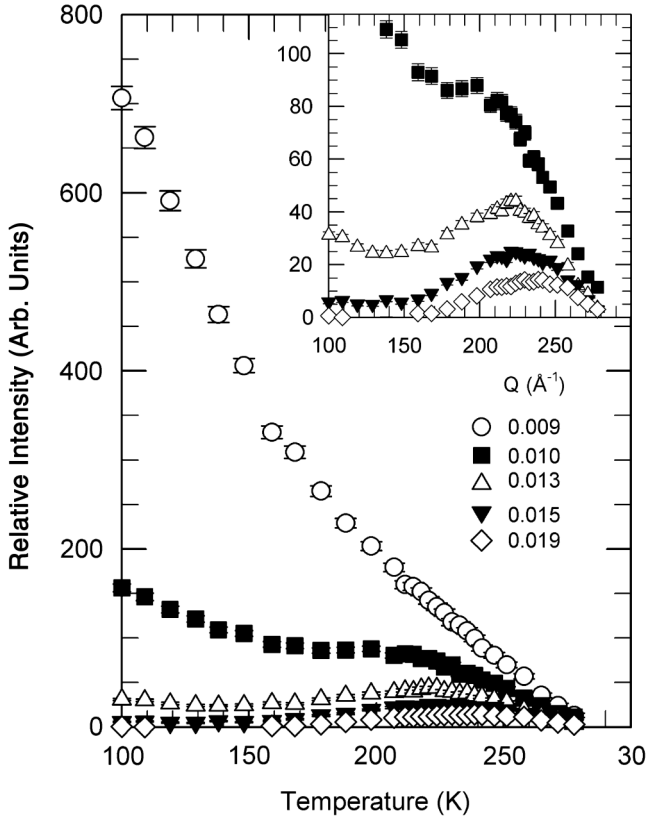

FIG. 1. Temperature dependence of the SANS intensity from $Y(Mn_{0.4}Fe_{0.6})_2$ for several values of Q as given in the legend. The inset shows details of the scattering intensity close to T_C.

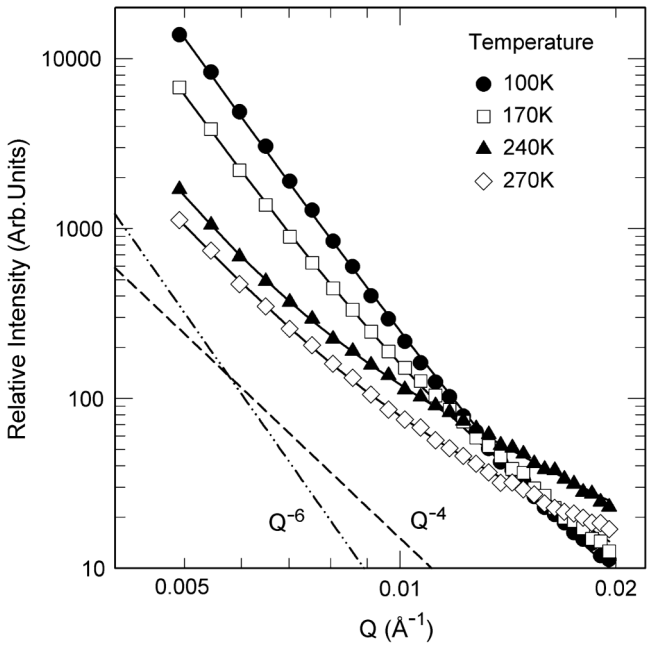

FIG. 2. Q dependence of the SANS intensity from $Y(Mn_{0.4}Fe_{0.6})_2$, at four different temperatures, plotted on logarithmic axes. The solid lines through the data points are least-squares fits of Eq. (3). Also shown are Q^{-4} (dashed line) and Q^{-6} (dash-dotted line) dependencies for comparison.

mum and minimum curvatures at any given point on the surface, by the relations $H = (k_1 + k_2)/2$ and $K = k_1 k_2$. For surfaces for which there is a significant difference between the mean and Gaussian curvatures, i.e., for extremely convoluted, dendritic or elongated surfaces, it is clear that the Q^{-6} Kirste-Porod contribution can be significant. The coefficient of the Q^{-6} term in Eq. (2) can therefore be interpreted as a measure of the asphericity ζ of the scattering surfaces within the Porod regime.

At first sight there might seem to be very little justification for applying a scattering model originally derived for a structural microemulsion to an inhomogeneous ferromagnet close to the percolation threshold. However, clear evidence for percolation clusters with a microemulsionlike morphology in $Y(Mn_{0.4}Fe_{0.6})_2$ is provided by a simple simulation of the intrinsic moment distributions and spin correlations based upon the near-neighbor rules proposed by Jian-Wang *et al.* [6] and described above.

For the simulation the spin exchange was modeled by a Yukawa-like function with a correlation range equal to the near-neighbor transition metal distance. This scalar field was converted to an isosurface at the level at which the spin exchange is equal to zero, thereby allowing the surface of the percolation clusters to be mapped using an implementation of the marching cubes algorithm [17], which also calculates the isosurface normals at each vertex of the resulting polygons. For a $3 \times 3 \times 3$ unit cell model, the surface generated 33 436 polygons on a cubic sampling grid with a point spacing of 0.36 Å. This sampling density appears to capture the surface geometry in sufficient detail, as shown in Fig. 3 where the resulting smooth but convoluted surfaces can be seen to bear a close resemblance to visualizations of structural microemulsion systems [18]. A numerical approximation for the asphericity ζ of the surface shown in Fig. 3 of $\sim 7.4 \times 10^{-4}$ has been calculated directly from the vertex positions and surface normals of the polygons.

Given the surface morphologies shown in Fig. 3, it is therefore perhaps not surprising that the scattering function

$$I(Q) = \frac{A}{\kappa^2 + Q^2} + \frac{B}{Q^4} + \frac{C}{Q^6} \tag{3}$$

provides an excellent description of the SANS from $Y(Mn_{0.4}Fe_{0.6})_2$ at all temperatures, as can be seen in Fig. 2.

In Eq. (3) we have incorporated the familiar Ornstein-Zernicke function to account for the ferromagnetic critical scattering, and find that the correlation range κ^{-1} diverges, as expected, at a Curie temperature of $T_C = 250 \pm 1$ K, in good agreement with the literature [10,19].

The final two terms in Eq. (3) are associated with the Kirste-Porod contributions, respectively. Fitting this function to the data enables us to extract the mean asphericity parameter of the cluster surface using $\zeta = C/B$. This definition ensures that the experimentally determined ζ is independent of the Porod and Kirste-Porod contrast terms and therefore of any normalization constants. The temperature dependence of ζ so obtained from fits of Eq. (3) to the $Y(Mn_{0.4}Fe_{0.6})_2$ SANS data is shown in Fig. 4.

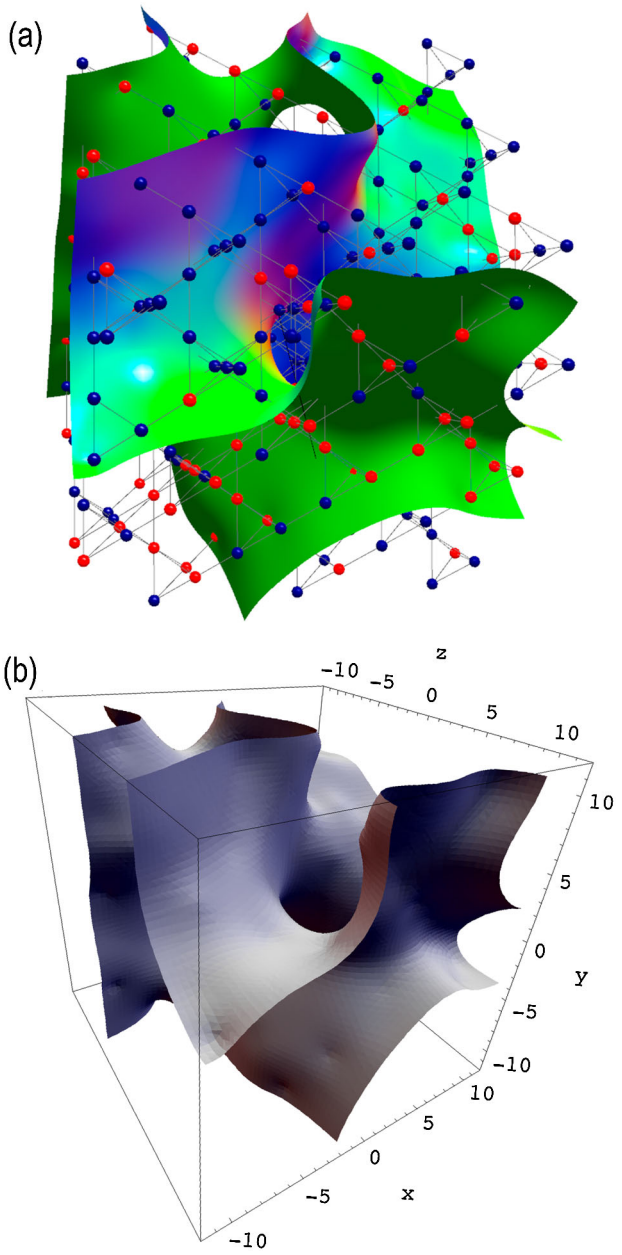

FIG. 3 (color online). Computer model of the percolation cluster surface, as described in the text. (a) shows smooth shading and with the atomic structure; the Fe atoms are light gray (bright red), the Mn atoms are dark gray (dark blue). (b) shows flat shading to show the sampling density. The axes dimensions are angstrom units.

At low temperatures the asphericity parameter of the ferromagnetic percolation clusters rises to a value of $\zeta \sim 4.4 \times 10^{-4}$, in surprisingly close agreement with that calculated from the simple spin correlation model described above. The asphericity, and by implication the shape of the percolation clusters, remains relatively constant to ap-

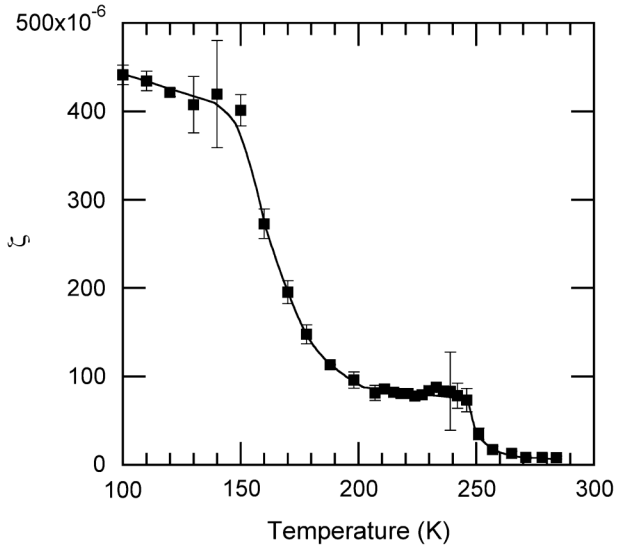

FIG. 4. Temperature dependence of the percolation cluster "asphericity" ζ in $Y(Mn_{0.4}Fe_{0.6})_2$. The solid line is a guide for the eye.

proximately 150 K, above which the asphericity decreases as the critical temperature ($T_C = 250$ K) is approached.

It therefore appears that the highly anomalous Q^{-6} dependence of the magnetic SANS from $Y(Mn_{0.4}Fe_{0.6})_2$ arises from ferromagnetic percolation clusters which have a well-defined but highly convoluted surface morphology closely resembling that found in structural microemulsions. Teubner's derivation of the Kirste-Porod scattering contributions from the interfaces in a bicontinuous structural microemulsion describes the observed SANS extremely well. This suggests that the distinct ferromagnetic cluster surfaces in $Y(Mn_{0.4}Fe_{0.6})_2$ are also smooth and nonfractal with a negligible interfacial thickness. This result is supported both qualitatively and quantitatively by our simple spin correlation model. In this respect the ferromagnetic percolation clusters embedded in an essentially antiferromagnetic $Y(Mn_{0.4}Fe_{0.6})_2$ matrix form a system which, in terms of scattering length density, is closely analogous to an immiscible suspension of water droplets in oil: in other words $Y(Mn_{0.4}Fe_{0.6})_2$ appears to be an example of a "spin emulsion." To our knowledge this is the first time such unusual spin emulsion morphology has been observed in any magnetic system.

Finally, the results and analysis presented here suggest that some caution may be necessary when applying the generalized magnetic SANS function of Eq. (1): in the limit at which the correlation length κ^{-1} approaches the resolution of the SANS instrument it is not possible to distinguish a squared Lorentzian scattering function, arising from random exchange or random anisotropy, from the Porod Q^{-4} form arising from cluster interfaces. The latter effect may be more significant than previously recognized.

We are very grateful to Professor S. H. Kilcoyne (Salford, U.K.) and Dr. J. R. Stewart (ISIS Facility, U.K.) for helpful discussions and for assistance during the experiments. P. M. B. would like to acknowledge financial support during experiments from the EPSRC, during analysis from NMI3, and currently from the European Strategy Forum on Research Infrastructures (ESFRI).

*bentley@ill.fr

[1] A. Aharony and E. Pytte, Phys. Rev. B **27**, 5872 (1983).
[2] B. D. Rainford, R. Cywinski, and S. J. Dakin, J. Magn. Magn. Mater. **140–144**, 805 (1995).
[3] R. Cywinski, S. H. Kilcoyne, and C. A. Scott, J. Phys. Condens. Matter **3**, 6473 (1991).
[4] S. Mondal, R. Cywinski, S. H. Kilcoyne, B. D. Rainford, and C. Ritter, Physica (Amsterdam) **180–181B**, 108 (1992).
[5] R. Cywinski, S. H. Kilcoyne, and C. Ritter, Appl. Phys. A **74**, s865 (2002).
[6] C. Jian-Wang, L. He-Lie, and Z. Quing-Qi, J. Phys. Condens. Matter **6**, 8903 (1994).
[7] H. Nagai, H. Yoshie, and A. Tsujimura, J. Phys. Soc. Jpn. **52**, 1122 (1983).
[8] H. Nagai, Hyperfine Interact. **51**, 1003 (1989).
[9] O. Moze, E. J. Lindley, B. D. Rainford, and D. MckPaul, J. Magn. Magn. Mater. **53**, 167 (1985).
[10] M. J. Besnus, A. Herr, K. L. Dang, P. Veillet, A. S. Schaafsma, I. Vincze, F. van der Woude, F. Mezei, and G. H. M. Calis, J. Phys. F **12**, 2393 (1982).
[11] G. Porod, Kolloid Z. **124**, 83 (1951).
[12] G. Porod, Kolloid Z. **125**, 51 (1952).
[13] P. J. McMahon, I. Snook, and E. Smith, J. Chem. Phys. **114**, 8223 (2001).
[14] H. D. Bale and P. W. Schmidt, Phys. Rev. Lett. **53**, 596 (1984).
[15] M. Teubner, J. Chem. Phys. **92**, 4501 (1990).
[16] R. von Kirste and G. Porod, Kolloid Z. **184**, 1 (1962).
[17] C. Bloyd, http://astronomy.swin.edu.au/pbourke/modelling/polygonise/.
[18] D. Choy and S.-H. Chen, Phys. Rev. E **63**, 021401 (2001).
[19] P. M. Bentley, Ph.D. thesis, School of Physics and Astronomy, University of Leeds, 2003.